

Integrating the full four-loop negative geometries and all-loop ladder-type negative geometries in ABJM theory

Zhenjie Li^a

^a*SLAC National Accelerator Laboratory, Stanford University, Stanford, CA 94309, USA*

E-mail: zhenjiel@slac.stanford.edu

ABSTRACT: The decomposition of the four-point ABJM amplituhedron into negative geometries produces a compact integrand of logarithmic of amplitudes such that the infrared divergence only comes from the last loop integral, from which we can compute the cusp anomalous dimension of the ABJM theory. In this note, we integrate $L - 1$ loop momenta of the L -loop negative geometries for all four-loop negative geometries and a special class of all-loop ladder-type negative geometries by a method based on Mellin transformation, and from these finite quantities we extract the corresponding contribution to the cusp anomalous dimension. We find that the infrared divergence of a box-type negative geometry at $L = 4$ is weaker than other negative geometries, then only tree-type negative geometries contribute to the cusp anomalous dimension at $L = 4$. For the all-loop ladder-type negative geometries, we prove and conjecture some recursive structures as integral equations in Mellin space and find that they cannot contribute zeta values like ζ_3, ζ_5 to the cusp anomalous dimension.

Contents

1	Introduction and review	1
1.1	Review of ABJM four-point amplituhedron and negative geometries	3
2	Integrating the 4-loop ABJM negative geometries	7
2.1	Star diagram	7
2.2	Box diagram	8
2.3	Ladder diagram	11
3	Cusp anomalous dimension from integrated results	12
4	Higher loop ladders	15
5	Discussions	19
A	Collection of useful 1-loop integrals	21
B	Function of 5-loop ladder	22

1 Introduction and review

The amplituhedron of planar $\mathcal{N} = 4$ super Yang-Mills theory (SYM) [1–3] is a surprising geometric structure, where the canonical forms of these positive geometries [4] encode all-loop, all-multiplicity scattering amplitudes in the theory. This discovery has spurred the exploration of analogous positive geometries in various other theories and contexts (see, for example, [5–12]). In [13], it is argued that by projecting both external and loop momenta to $D = 3$ of four-point amplituhedron in $\mathcal{N} = 4$ sYM, we get the amplituhedron of four-point integrands in $\mathcal{N} = 6$ Chern-Simons-matter theory, or ABJM theory [14, 15], and then the construction is generalized to any multiplicity in [16].

In [17], the four-point amplituhedron of planar $\mathcal{N} = 4$ sYM is decomposed into the so-called *negative geometries*, where the sum of all connected negative geometries naturally gives the integrand of logarithmic of the 4-point amplitude. Another important feature of this decomposition is that the infrared (IR) structure of integrated connected negative geometry is quite mild, it can only has at most ϵ^{-2} (ϵ^{-2L} for general L -loop diagrams) divergence after integrating all loop momenta in the dimensional regularization $D = 4 - 2\epsilon$, which is in fact a one-loop divergence. Therefore, if we first fix one loop momentum not to integrate and integrate the other loop momenta in a connected negative geometry, we will get an IR finite object, which has the dual conformal symmetry after dividing a suitable factor, or equivalently which is a function in

$$z = \frac{(\ell - x_2)^2(\ell - x_4)^2(x_1 - x_3)^2}{(\ell - x_1)^2(\ell - x_3)^2(x_2 - x_4)^2}. \quad (1.1)$$

where the dual momentum x_i is defined as $x_{i+1} - x_i = p_i$ and $x_5 = x_1$. For $\mathcal{N} = 4$ sYM theory, this IR finite object is calculated up to $L = 4$ [17–24]. It is also remarkable in [17] that a subset of all-loop negative geometries can be completely solved by differential equations relating these negative geometries.

For the four-point ABJM amplituhedron, we can also investigate the similar decomposition into negative geometries. In [13], it shows that we can further decompose connected negative geometries according to the emergent causal structure, and then most of geometries cancel in the final decomposition, which leads a huge simplification comparing to the $\mathcal{N} = 4$ sYM case. For example, the integrand of four-loop log of amplitude in ABJM theory is given by *only* 4 distinct negative geometries (with permutation) which is represent by *bipartite* graphs

$$\tilde{\Omega}_4 = -4 \begin{array}{c} \bullet \\ / \quad | \quad \backslash \\ \circ \quad \circ \quad \circ \end{array} - 4 \begin{array}{c} \circ \\ / \quad | \quad \backslash \\ \bullet \quad \bullet \quad \bullet \end{array} - 24 \circ \bullet \circ \bullet + 6 \begin{array}{c} \circ \quad \bullet \\ | \quad | \\ \bullet \quad \circ \end{array}, \quad (1.2)$$

where each node of the diagram represents a loop. For each ABJM negative geometry, it shares the nice IR structure as the $\mathcal{N} = 4$ sYM negative geometry. Similarly, each negative geometry defines a IR finite object after integrating $L - 1$ loop momenta out of L loops, which is calculated up to $L = 3$ [25, 26].

For both $\mathcal{N} = 4$ sYM and ABJM theory, the above IR finite object is in fact related to the correlation function Wilson loop with a Lagrangian insertion by Wilson loop-amplitude duality (see *e.g.* [27–37]). The four-point amplitudes is related to the polygon Wilson loop with 4 vertex x_1, \dots, x_4 :

$$\log W_4(x_1, x_2, x_3, x_4) \sim \log \left(A_4 / A_4^{(0)} \right), \quad (1.3)$$

where $A_4^{(0)}$ is the tree-level amplitude, and this duality also holds at the integrand level. According to the Lagrangian insertion formula $g^2 \partial_{g^2} \langle \mathcal{O} \rangle = -i \int d^D \ell \langle \mathcal{O} \mathcal{L}(\ell) \rangle$ (g^2 is the expansion parameter), the important IR-finite quantity from integrating all but one loop of the negative geometry is related to the Wilson loop with a Lagrangian insertion [19, 22, 24, 38].

The Wilson loop $\log W_4$ has ultraviolet (UV) divergence, which corresponds to propagating gluons between two adjacent sides of the Wilson loop around a cusp perturbatively. To regularize this divergence, one can introduce a renormalization factor Z_{cusp} , and therefore define the a cusp anomalous dimension as $\Gamma_{\text{cusp}} = \mu \partial_\mu Z_{\text{cusp}}$, where μ is the renormalization scale of the theory. The cusp anomalous dimension Γ_{cusp} appears in $\log W_4$ as

$$\log \langle W_4 \rangle = -2 \sum_{L=1}^{\infty} \frac{\lambda^L \Gamma_{\text{cusp}}^{(L)}}{(L\epsilon)^2} + \mathcal{O}(\epsilon^{-1})$$

in the dimensional regularization. Therefore, both for the $\mathcal{N} = 4$ sYM [17] and the ABJM [25, 26] theory, we can extract the cusp anomalous dimension from the ϵ^{-2} order of IR divergence of the logarithm of the 4-point amplitude by the Wilson loop-amplitude duality. Based this method, the two-loop cusp anomalous dimension of the ABJM theory

is computed in [25, 26]. While as proposed in [25, 26], there is no contribution to the cusp anomalous dimension from negative geometry with an odd number of loops, so the next leading order of the cusp anomalous dimension is at $L = 4$.

In this note, we are mainly interested in integrating three loop momenta out of 4 loops for each negative geometry in eq.(1.2) in ABJM theory, which can be used to calculate the 4-loop cusp anomalous dimension $\Gamma_{\text{cusp}}^{(4)}$ of the ABJM theory. The note is organized as follows. In the next subsection, we will review ABJM four-point amplituhedron and negative geometries and gives the explicit integrand for each bipartite graph in eq.(1.2). In section 2, we will integrate three loop momenta out of 4 loops for each diagram based on Mellin method. In section 3, we extract the cusp anomalous dimension by further integrating the last loop momentum, and we find that the box diagram

$$\int \prod_{i=1}^4 d^3 \ell_i \quad \begin{array}{ccc} & 4 & 3 \\ & \circ & \bullet \\ & | & | \\ \bullet & & \circ \\ 1 & & 2 \end{array} = O(\epsilon^{-1}) \quad (1.4)$$

does not contribute to the cusp anomalous dimension, and we prove it by looking at the integrand in collinear regions. In section 4, we consider a subset of all-loop (ladder-type) negative geometries, and we present a recursion relation based Mellin method, and conjecture that this type of negative geometries only contributes the power of π and no other zeta values like ζ_3, ζ_5 to the cusp anomalous dimension.

1.1 Review of ABJM four-point amplituhedron and negative geometries

Roughly speaking, the ABJM amplituhedron is defined by reducing the dimension of the 4 dimensional $\mathcal{N} = 4$ sYM amplituhedron. The reducing is archived by imposing a universal projection for each external and loop momentum. For imposing this kinematics condition, we first review the kinematics of both $\mathcal{N} = 4$ sYM and ABJM theories and fix the corresponding notations.

For planar massless theories with external momentum $\{p_i : 1 \leq i \leq n\}$, it is convenient to introduce dual momentum (or dual point) $\{x_i : 1 \leq i \leq n\}$, defined through $p_i = x_{i+1} - x_i$ (with $x_{n+1} = x_1$) [39], and any physical quantities in these theories are functions in planar kinematics variables

$$(x_i - x_j)^2 = (p_i + p_{i+1} + \dots + p_{j-1})^2. \quad (1.5)$$

To linearize the conformal group of dual space (dual conformal group), we embed the dual space $\mathbb{R}^{d,1}$ into $\mathbb{R}^{d+1,2}$ with two extra dimensions [40, 41], where the dual conformal group becomes $\text{SO}(d+1, 2)$. Each dual momentum x^μ is sent to a vector $X = (x^2, 1, x^\mu) \in \mathbb{R}^{d+1,2}$, and the metric of $\mathbb{R}^{d+1,2}$ is

$$\eta = \begin{pmatrix} 0 & 1 & & \\ 1 & 0 & & \\ & & & -2\eta^{\mu\nu} \end{pmatrix},$$

where $\eta^{\mu\nu}$ is the spacetime metric. The basic $\text{SO}(4, 2)$ invariants are inner products of two vectors in the embedding space. We denote the inner product of two vectors X and Y as

$(X \cdot Y)$, and define $X_i := (x_i^2, 1, x_i^\mu)$ and the shorthand

$$(i \cdot j) := (X_i \cdot X_j) = (x_i - x_j)^2. \quad (1.6)$$

Since the square of $X = (x^2, 1, x^\mu)$ vanishes, *i.e.* $(X \cdot X) = x^2 - x^2 = 0$, the dual space can be identified more intrinsically as a quadric defined by $(X \cdot X) = 0$ module the identification $X \sim \alpha X$ for $\alpha \neq 0$. Dual conformal invariants (DCI) of dual momentum should be built from inner product of these X 's, and it can only be the function of cross-ratios of inner products.

For the four-dimensional spacetime, such X can be further parameterized by a wedge product of two twistors (a bi-twistor) $A \wedge B := (AB)$ in a twistor space \mathbb{P}^3 , such twistors call called momentum twistors [42], and the dimension of space of bi-twistors is also $\binom{4}{2} - 2 = 6 - 2 = 4$. The inner product now corresponds to the wedge product,

$$(X \cdot X') \propto (AB) \wedge (A'B') = A \wedge B \wedge A' \wedge B' =: \langle ABA'B' \rangle,$$

and the proportionality factors will finally cancel in any dual conformal invariants. Since $p_i = x_{i+1} - x_i$ is massless, or $(i, i+1) = 0$, each X_i can be chosen as a bi-twistor $(Z_{i-1}Z_i)$ (with $Z_0 = Z_n$) for n momentum twistors $\{Z_i\}_{i=1, \dots, n}$, and each loop momentum ℓ_i corresponds to a bi-twistor (A_iB_i) . We also introduce a shorthand

$$\langle ijkl \rangle := \langle Z_i Z_j Z_k Z_l \rangle, \quad \langle \ell_i kl \rangle := \langle A_i B_i Z_k Z_l \rangle, \quad \langle \ell_i \ell_j \rangle := \langle A_i B_i A_j B_j \rangle. \quad (1.7)$$

However, for the three-dimensional spacetime, we cannot view a dual momentum X as a bi-twistor in any twistor space \mathbb{P}^k , the dimension $\binom{k}{2} - 2$ will never be 3. In [43], a nice way to represent 3D kinematics by taking a projection from 4D momentum twistor was proposed as follows. We first go back the the embedding space, by setting a vector Ω with $(\Omega, \Omega) = 1$, we require that all dual points and loop momentum are orthogonal to Ω , *i.e.*

$$(X_i \cdot \Omega) = 0, \quad (\ell \cdot \Omega) = 0,$$

and then the conformal group is naturally reduced to $\text{SO}(2, 3)$. In twistor space, this is equivalent to impose a *symplectic condition* on both external bi-twistor $(Z_a Z_{a+1})$ and loop variables $\ell_i \sim (A_i B_i)$ that

$$\Omega_{IJ} Z_a^I Z_{a+1}^J = \Omega_{IJ} A_i^I B_i^J = 0, \quad \text{with a choosen } \Omega = \begin{pmatrix} & & & 1 \\ & & -1 & \\ & 1 & & \\ -1 & & & \end{pmatrix} \quad (1.8)$$

where $I = 1, \dots, 4$ is the index of the twistor space \mathbb{P}^3 .

Now we can give the definition of the ABJM amplituhedron for four points [13], the generalization to n points see [16]. The four-point ABJM amplituhedron is defined by

$$\langle \ell_i 12 \rangle, \langle \ell_i 23 \rangle, \langle \ell_i 34 \rangle, \langle \ell_i 14 \rangle < 0, \langle \ell_i 13 \rangle, \langle \ell_i 24 \rangle > 0, \langle \ell_i \ell_j \rangle < 0, \quad (1.9)$$

all defined on the support of eq.(1.8), and its canonical form will produce the all-loop ABJM integrand. Note that, there is an important subtlety is that $\langle 1234 \rangle < 0$ for real Z 's

satisfying the symplectic condition, so we need to flip the overall sign for the definition of the $D = 4$ amplituhedron [1].

When computing the canonical form, $\langle \ell_i \ell_j \rangle < 0$ is the most non-trivial condition which mix different loops. In [17], there is a new decomposition for the four-point amplituhedron [2] based on a simple fact that

$$\Omega(C, \langle \ell_i \ell_j \rangle > 0) + \Omega(C, \langle \ell_i \ell_j \rangle < 0) = \Omega(C),$$

where Ω is the canonical form and C is the set of the other inequalities. Therefore, just replacing $\Omega(C_j, \langle \ell_i \ell_j \rangle < 0)$ by $\Omega(C) - \Omega(C_i, \langle \ell_i \ell_j \rangle > 0)$ for all possible $\langle \ell_i \ell_j \rangle$, we can decompose the geometry to geometries with only “mutual negativity” conditions $\langle \ell_i \ell_j \rangle > 0$ such that the L -loop geometry \mathcal{A}_L can be decomposed into

$$\mathcal{A}_L = \sum_g (-)^{E(g)} \mathcal{A}(g), \quad (1.10)$$

where we use a graph g with L nodes to label a geometry $\mathcal{A}(g)$ and sum over all possible (maybe disconnected) graphs without 2-cycles. The node of a graph denote a loop, and a edge between two nodes i and j means we need to apply the condition $\langle \ell_i \ell_j \rangle > 0$. For each graph, we need less conditions $\langle \ell_i \ell_j \rangle > 0$, so it will be easier to compute its canonical form. Furthermore, it suffices to consider all *connected* graphs, whose (signed) sum gives the geometry for the logarithm of amplitudes [17].

A further simplification [13] occurs in 3D ABJM amplituhedron, most of these geometries do not contribute at all. We can further decompose $\langle \ell_i \ell_j \rangle > 0$ into two regions which gives two possible directions on each edge, and we need to sum over all possible directed graphs. In such decomposition, the condition given by $i \rightarrow j \rightarrow k$ implies the condition $i \rightarrow k$, so different graphs can represent the same geometry, which leads a huge cancellation in the signed summation. Finally, we only need to sum over all *bipartite* graphs. A bipartite graph is a directed graph with only sinks and sources, we will use black/white node to denote a source/sink vertex and omit all directions on edges in a bipartite. Therefore, the canonical form of L -loop amplitude Ω_L and log of L -loop amplitude $\tilde{\Omega}_L$ read

$$\Omega_L = \sum_{\text{bipartite } g} (-)^{E(g)} \Omega(g), \quad \tilde{\Omega}_L = \sum_{\substack{\text{connected} \\ \text{bipartite } g}} (-)^{E(g)} \Omega(g). \quad (1.11)$$

For example, for the 3-loop case, only the chain graph contributes, *i.e.*

$$\tilde{\Omega}_3 = \begin{array}{c} 1 \\ \bullet \end{array} - \begin{array}{c} 2 \\ \bullet \end{array} - \begin{array}{c} 3 \\ \bullet \end{array} + 5 \text{ permutations}, \quad (1.12)$$

and only the two kinds of tree graphs and the box contribute for $\tilde{\Omega}_4$, *i.e.*

$$\tilde{\Omega}_4 = -4 \begin{array}{c} \bullet \\ / \quad \backslash \\ \circ \quad \circ \end{array} - 4 \begin{array}{c} \bullet \\ / \quad \backslash \\ \bullet \quad \bullet \end{array} - 24 \begin{array}{c} \circ \quad \bullet \\ | \quad | \\ \bullet \quad \circ \end{array} + 6 \begin{array}{c} \circ \quad \bullet \\ | \quad | \\ \bullet \quad \circ \end{array} \quad (1.13)$$

This simplification becomes more significant with L increasing. For $L = 2, \dots, 7$, the number of topologies for connected graphs are 1, 2, 6, 21, 112, 853, but that of bipartite

topologies decrease to 1, 1, 3, 5, 17, 44. All canonical forms of negative geometries up to $L = 5$ have been computed [13]. We here list all graphs and their integrands up to $L = 4$,

$$\bullet = \frac{c\epsilon_1}{s_1 t_1}, \quad \bullet \text{---} \circ = \frac{2c^2}{s_1 t_2 D_{1,2}}, \quad \bullet \text{---} \circ \text{---} \bullet = \frac{4c^2 \epsilon_2}{s_1 t_2 s_3 D_{1,2} D_{2,3}} \quad (1.14)$$

$$\bullet \text{---} \circ \text{---} \bullet \text{---} \circ = \frac{8c^2 \epsilon_2 \epsilon_3}{D_{1,2} D_{2,3} D_{3,4} s_1 t_2 s_3 t_4}, \quad \begin{array}{c} \bullet \\ | \\ \circ \\ | \\ \circ \\ | \\ \circ \end{array} = \frac{8c^3 t_1}{D_{1,2} D_{1,3} D_{1,4} s_1 t_2 t_3 t_4} \quad (1.15)$$

$$\begin{array}{c} \bullet \\ | \\ \circ \\ | \\ \circ \\ | \\ \circ \end{array} = 4 \frac{4\epsilon_1 \epsilon_2 \epsilon_3 \epsilon_4 - c(\epsilon_1 \epsilon_3 N_{24}^t + \epsilon_2 \epsilon_4 N_{13}^s) - c^2 N_{1,2,3,4}^{\text{cyc}}}{D_{1,2} D_{2,3} D_{3,4} D_{4,1} s_1 t_2 s_3 t_4} \quad (1.16)$$

where

$$D_{i,j} = -\langle \ell_i \ell_j \rangle, \quad s_i = \langle \ell_i 12 \rangle \langle \ell_i 34 \rangle, \quad t_i = \langle \ell_i 23 \rangle \langle \ell_i 14 \rangle, \quad c = \langle 1234 \rangle, \quad \epsilon_i = \sqrt{\langle 1234 \rangle \langle \ell_i 13 \rangle \langle \ell_i 24 \rangle}$$

and

$$\begin{aligned} N_{13}^s &:= \langle \ell_1 12 \rangle \langle \ell_3 34 \rangle + \langle \ell_3 12 \rangle \langle \ell_1 34 \rangle \\ N_{24}^t &:= -\langle \ell_2 41 \rangle \langle \ell_4 23 \rangle - \langle \ell_4 41 \rangle \langle \ell_2 23 \rangle \\ N_{i,j,k,l}^{\text{cyc}} &:= \langle \ell_i 12 \rangle \langle \ell_j 34 \rangle \langle \ell_k 12 \rangle \langle \ell_l 34 \rangle + \text{cyc}(1, 2, 3, 4). \end{aligned}$$

Other graphs with white and black vertex interchanged can be obtained by $s \leftrightarrow t$ (or equivalently $X_1 \leftrightarrow X_2, X_3 \leftrightarrow X_4$).

To translate expressions in momentum twistors to embedding space, we give a dictionary here:

$$\begin{aligned} \frac{\epsilon_i}{c} &\rightarrow \frac{\epsilon(1, 2, 3, 4, \ell_i)}{-(1 \cdot 3)(2 \cdot 4)}, \quad \frac{s_i}{c} \rightarrow \frac{(\ell_i \cdot 2)(\ell_i \cdot 4)}{(2 \cdot 4)}, \quad \frac{t_i}{c} \rightarrow \frac{(\ell_i \cdot 1)(\ell_i \cdot 3)}{(1 \cdot 3)}, \\ D_{i,j} &\rightarrow -(\ell_i \cdot \ell_j), \quad c \rightarrow -(1 \cdot 3) \text{ or } (2 \cdot 4), \end{aligned} \quad (1.17)$$

where ϵ is the totally anti-symmetric tensor in the embedding space $\mathbb{R}^{2,3}$:

$$\epsilon(1, 2, 3, 4, \ell_i) := \epsilon_{IJKLM} X_1^I X_2^J X_3^K X_4^L (\ell_i)^M,$$

which is normalized as

$$\epsilon(y_1, y_2, y_3, y_4, y_5) \epsilon(z_1, z_2, z_3, z_4, z_5) = -\det((y_i \cdot z_j))/2,$$

and we need to choose c to be $-(1 \cdot 3)$ or $(2 \cdot 4)$ to make integrals dual conformal invariant in embedding space.

In this note, we focus on calculating the finite quantity of ABJM four-point amplituhedron

$$\mathcal{W}_L(\ell, 1, 2, 3, 4) := \int \prod_{i=2}^L \frac{d^3 \ell_i}{i\pi^{3/2}} \tilde{\Omega}_L, \quad (1.18)$$

which depends on the last loop ℓ_1 and external points; after stripping off a non-DCI prefactor it becomes function of a single cross-ratio

$$z = \frac{(\ell \cdot 2)(\ell \cdot 4)(1 \cdot 3)}{(\ell \cdot 1)(\ell \cdot 3)(2 \cdot 4)}. \quad (1.19)$$

This will be the main target of loop integrations for ABJM amplituhedron.

2 Integrating the 4-loop ABJM negative geometries

In this section, we consider the corresponding $\mathcal{W}_L(\ell, 1, 2, 3, 4)$ for $L = 4$ negative geometries whose integrands are listed in eq.(1.15) and (1.16), and the log of amplitude is given by

$$\tilde{\Omega}_4 = -4 \begin{array}{c} \bullet \\ / \quad | \quad \backslash \\ \circ \quad \circ \quad \circ \end{array} - 4 \begin{array}{c} \circ \\ / \quad | \quad \backslash \\ \bullet \quad \bullet \quad \bullet \end{array} - 24 \circ \bullet \circ \bullet + 6 \begin{array}{c} \circ \quad \bullet \\ | \quad | \\ \bullet \quad \circ \end{array} . \quad (2.1)$$

To perform the integration of loop momentum and consider the resummation, we follow the normalization in [26]. The expansion of the log of the integrand with respect to 't Hooft coupling $\lambda = N/k$ is

$$\mathcal{L} = \sum_{L=1}^{\infty} \lambda^L \mathcal{L}_L = \sum_{L=1}^{\infty} \frac{1}{L!} \left(\frac{i}{2\sqrt{\pi}} \right)^L \lambda^L \tilde{\Omega}_L = \sum_g \frac{1}{L_g!} \left(\frac{i}{2\sqrt{\pi}} \right)^{L_g} \lambda^{L_g} (-1)^{E_g} \tilde{\Omega}_g, \quad (2.2)$$

where we sum over all connected bipartite graphs g with L_g nodes and E_g edges in the last summation. After performing the loop integration of ℓ_2, \dots , we define

$$F_g = \frac{1}{L_g!} \left(\frac{i}{2\sqrt{\pi}} \right)^{L_g} \left[\frac{1}{\sqrt{\pi}} \left(\frac{(1 \cdot 3)(2 \cdot 4)}{(\ell \cdot 1)(\ell \cdot 3)(\ell \cdot 2)(\ell \cdot 4)} \right)^{3/4} \right]^{-1} \int \prod_{i=2}^L \frac{d^3 \ell_i}{i\pi^{3/2}} \tilde{\Omega}_g, \quad (2.3)$$

where the prefactor is introduced to cancel the dual conformal weight of the left loop momentum such that F_g is a dual conformal invariant¹, or is a function in z .

We will separate the calculation into three type of diagrams in three subsections: star, box and ladder. We here first collect all results:

$$F_{\text{star}} = -\frac{\pi^3}{12} (z^{-1/4} + z^{1/4}), \quad (2.4)$$

$$F_{\text{box}} = \frac{\pi^3}{32} \left(\frac{2}{3} z^{-1/4} + 2z^{1/4} - \frac{4}{\pi^2} z^{-1/4} (1+z) f(z) \right) + (z \leftrightarrow 1/z), \quad (2.5)$$

$$F_{\text{ladder}} = -\frac{\pi^3}{8} z^{-1/4} \left(1 + \frac{\log(z/4)^2}{2\pi^2} + \frac{(1+z)f(z)}{\pi^2} \right) + (z \leftrightarrow z^{-1}), \quad (2.6)$$

where $f(z)$ is a weight-2 polylogarithm defined in eq.(2.15).

2.1 Star diagram

The integrand for star diagram

$$S = \begin{array}{c} 1 \\ \bullet \\ / \quad | \quad \backslash \\ \circ \quad \circ \quad \circ \\ 2 \quad 3 \quad 4 \end{array} = 8c^3 \frac{t_1}{D_{1,2} D_{1,3} D_{1,4} s_1 t_2 t_3 t_4} \quad (2.7)$$

$$= -8 \frac{(\ell_1 \cdot 1)(\ell_1 \cdot 3)(2 \cdot 4)}{(\ell_1 \cdot 2)(\ell_1 \cdot 4)(1 \cdot 3)} \prod_{i=2}^4 \frac{(1 \cdot 3)}{(\ell_1 \cdot \ell_i)(\ell_i \cdot 1)(\ell_i \cdot 3)},$$

¹The prefactor for the negative geometry with an odd number of loops is different, see [25, 26].

we further use a subscript to denote which node is left to unintegrated,

$$S_i = \left[\frac{1}{\sqrt{\pi}} \left(\frac{(2 \cdot 4)(1 \cdot 3)}{(\ell \cdot 2)(\ell_1 \cdot 4)(\ell \cdot 1)(\ell \cdot 3)} \right)^{3/4} \right]^{-1} \int_{\{1,2,3,4\} \setminus \{i\}} S,$$

and unlabeled ℓ or z always corresponds to unintegrated node.

It is easy to perform the loop integral for S by recursively using the one-loop scale triangle integral in 3D

$$\int_{\ell} \frac{1}{(\ell \cdot a)(\ell \cdot b)(\ell \cdot c)} = \frac{\pi^{3/2}}{\sqrt{(a \cdot b)(b \cdot c)(c \cdot a)}}, \quad (2.8)$$

and we get that

$$S_1 = -8\pi^5 z^{-1/4}, \quad S_2 = S_3 = S_4 = -8\pi^5 z^{1/4}.$$

and

$$F_S = 4 \int_{\text{star}} = \frac{1}{4!} \left(\frac{i}{2\sqrt{\pi}} \right)^4 (S_1 + S_2 + S_3 + S_4) = -\frac{1}{48} \pi^5 (z^{-1/4} + 3z^{1/4}).$$

Similarly, the contribution from the other star diagram

$$\bar{S} = \int_{\text{star}} \quad (2.9)$$

is simply given by taking $z \rightarrow 1/z$ for S , so

$$F_{\bar{S}} = -\frac{1}{48} \pi^5 (z^{1/4} + 3z^{-1/4}).$$

The full star contribution is just

$$F_{\text{star}} = F_S + F_{\bar{S}} = -\frac{\pi^3}{12} (z^{-1/4} + z^{1/4}). \quad (2.10)$$

2.2 Box diagram

The integration of 4-loop box diagram is much more difficult than the star diagram. The integrand is

$$B = \int_{\text{box}} = 4 \frac{4\epsilon_1\epsilon_2\epsilon_3\epsilon_4 - c(\epsilon_1\epsilon_3 N_{24}^t + \epsilon_2\epsilon_4 N_{13}^s) - c^2 N_{1,2,3,4}^{\text{cyc}}}{D_{1,2} D_{2,3} D_{3,4} D_{4,1} s_1 t_2 s_3 t_4}$$

where

$$\begin{aligned} N_{13}^s &:= \langle \ell_1 12 \rangle \langle \ell_3 34 \rangle + \langle \ell_3 12 \rangle \langle \ell_1 34 \rangle \\ N_{24}^t &:= -\langle \ell_2 41 \rangle \langle \ell_4 23 \rangle - \langle \ell_4 41 \rangle \langle \ell_2 23 \rangle \\ N_{i,j,k,l}^{\text{cyc}} &:= \langle \ell_i 12 \rangle \langle \ell_j 34 \rangle \langle \ell_k 12 \rangle \langle \ell_l 34 \rangle + \text{cyc}(1, 2, 3, 4), \end{aligned}$$

where $\text{cyc}(1, 2, 3, 4)$ indicates cyclic rotations of dual points $12 \rightarrow 23 \rightarrow 34 \rightarrow 41$. We want to calculate

$$B_1 = \left(\frac{(2 \cdot 4)\sqrt{(1 \cdot 3)}}{(\ell_1 \cdot 2)(\ell_1 \cdot 4)\sqrt{(\ell_1 \cdot 1)(\ell_1 \cdot 3)}} \right)^{-1} \int_{\ell_2, \ell_3, \ell_4} B,$$

where the new prefactor is just

$$\frac{(2 \cdot 4)\sqrt{(1 \cdot 3)}}{(\ell \cdot 2)(\ell \cdot 4)\sqrt{(\ell \cdot 1)(\ell \cdot 3)}} = \left(\frac{(1 \cdot 3)(2 \cdot 4)}{(\ell \cdot 1)(\ell \cdot 3)(\ell \cdot 2)(\ell \cdot 4)} \right)^{3/4} z^{-1/4}. \quad (2.11)$$

We first expand the integrand and integrate loop 2 and loop 4, which is symmetric and gives the same result. There're two types of 1-loop integrals when integrating loop 2 and 4, the one is scale triangle

$$\int_{\ell} \frac{1}{(\ell \cdot a)(\ell \cdot b)(\ell \cdot c)} = \frac{\pi^{3/2}}{\sqrt{(a \cdot b)(b \cdot c)(c \cdot a)}}$$

and the other is a one-loop box integral with a numerator $N[\ell]$,

$$\int_{\ell} \frac{N[\ell]}{(\ell \cdot \ell_1)(\ell \cdot \ell_3)(\ell \cdot 1)(\ell \cdot 3)} = \pi^{3/2} \frac{N[\ell_1]/\sqrt{(\ell_1 \cdot 1)(\ell_1 \cdot 3)} + N[\ell_3]/\sqrt{(\ell_3 \cdot 1)(\ell_3 \cdot 3)}}{\sqrt{(1 \cdot 3)(\ell_1 \cdot \ell_3)} + \sqrt{(\ell_1 \cdot 3)(\ell_3 \cdot 1)} + \sqrt{(\ell_1 \cdot 1)(\ell_3 \cdot 3)}},$$

where $N[\ell]$ is linear in dual momentum ℓ and $N[1] = N[3] = 0$, for example, $N[\ell]$ could be ϵ_{ℓ} or $(\ell \cdot 2)$ or $(\ell \cdot 4)$. Therefore, with expanding the numerator by

$$\epsilon(y_1, y_2, y_3, y_4, y_5)\epsilon(z_1, z_2, z_3, z_4, z_5) = -\det((y_i \cdot z_j))/2,$$

we get that

$$\int_{\ell_2, \ell_4} B = \frac{P}{H^2} + Q,$$

where P, Q are rational functions of scale products and ϵ 's (*i.e.* they can expand as sums of monomials of scale products and ϵ 's), and

$$H := \sqrt{(1 \cdot 3)(\ell_1 \cdot \ell_3)} + \sqrt{(\ell_1 \cdot 3)(\ell_3 \cdot 1)} + \sqrt{(\ell_1 \cdot 1)(\ell_3 \cdot 3)}.$$

A monomial of scale products and ϵ 's is just a 1-loop integrand and is easy to work out, so we can calculate $\int_{\ell_3} Q$.

For calculating $\int_{\ell_3} P/H^2$, we introduce a inverse Mellin transform (which can be seen as an inverse Feynman parameterization) for $1/H^2$

$$\frac{1}{(A + B + C)^2} = \int_{\gamma_u, \gamma_v} \frac{du}{2\pi i} \frac{dv}{2\pi i} A^{-u} B^{-v} C^{-w} \frac{\Gamma(u)\Gamma(v)\Gamma(w)}{\Gamma(u+v+w)},$$

where $u + v + w = 2$, and contours γ_u, γ_v are defined that $\text{Re}(u) > 0, \text{Re}(v) > 0, \text{Re}(w) > 0$. Now we can first perform the ℓ_3 -integral for P/H^2 and then consider the inverse Mellin transform, the ℓ_3 -integrand is a sum of 1-loop integrals in the following form

$$\int_{\ell} \frac{N[\ell]^{n_0}}{(\ell \cdot 1)^{n_1} (\ell \cdot 2)^{n_2} (\ell \cdot 3)^{n_3} (\ell \cdot 4)^{n_4} (\ell \cdot \ell_1)^{n_5}},$$

where $n_0 = 0, 1$ and $n_1 + \dots + n_5 = 3 + n_0$, so we can introduce Feynman parameters a_1, \dots, a_5 (a_5 for $(\ell \cdot \ell_1)$) for each propagator and perform the loop integral. The result of this integral can be found in the Appendix.

Therefore, we get that

$$\begin{aligned} & \frac{\pi^{-9/2}}{4} \left(\frac{(2 \cdot 4) \sqrt{(1 \cdot 3)}}{(\ell_1 \cdot 2)(\ell_1 \cdot 4) \sqrt{(\ell_1 \cdot 1)(\ell_1 \cdot 3)}} \right)^{-1} \int_{\ell_2, \ell_3, \ell_4} B \\ &= -\frac{2}{\sqrt{z}} + \frac{2}{3} + (1+z) \left(\frac{4}{\pi^2} - \frac{16 \log(2)}{\pi^2} \right) + (1+z)(2+z)I_1 + (1+z)(I_2 + I_3), \end{aligned} \quad (2.12)$$

where

$$\begin{aligned} I_1 &= \frac{4}{\pi^{3/2}} \int_{\gamma_u, \gamma_v} \frac{du}{2\pi i} \frac{dv}{2\pi i} \int_{\mathbb{R}_+^2} da_3 da_4 \frac{(a_3 + 1)^{-\frac{v}{2}} (a_3 + a_4)^{\frac{v}{2} - \frac{3}{2}} a_3^{\frac{w}{2} - 1} \Gamma(u) \Gamma(v) \Gamma(w) \Gamma(\frac{3}{2} - \frac{v}{2})}{(a_4 + z) \Gamma(\frac{u}{2} + 1) \Gamma(w/2)}, \\ I_2 &= \frac{8}{\pi^{3/2}} \int_{\gamma_u, \gamma_v} \frac{du}{2\pi i} \frac{dv}{2\pi i} \int_{\mathbb{R}_+^2} da_3 da_4 \frac{(a_3 + 1)^{\frac{1}{2} - \frac{v}{2}} (a_3 + a_4)^{\frac{v}{2} - 1} a_3^{\frac{w}{2} - \frac{3}{2}} \Gamma(u) \Gamma(v) \Gamma(w) \Gamma(1 - \frac{v}{2})}{(a_4 + z) \Gamma(\frac{u}{2} + 1) \Gamma(w/2)}, \\ I_3 &= - \int_{\mathbb{R}_+^2} da_3 da_4 \frac{2}{\pi^2 \sqrt{a_3} \sqrt{a_3 + 1} (a_3 + a_4) (a_4 + z)}, \end{aligned}$$

and the contour here is

$$\gamma_u = \frac{1}{3} + i\mathbb{R}, \quad \gamma_v = \frac{1}{4} + i\mathbb{R}.$$

Note that we left two Feynman parameters to integrate later because if we directly integrate it, we will meet hypergeometric functions and it's very difficult to perform the inverse Mellin transform for it. However, we can introduce another Mellin transform for $1/(a_4 + z)$ to avoid this difficulty so that integration of a_3 and a_4 only produces Γ functions, and then the integration of the left u and v also becomes standard. Finally we get that

$$\begin{aligned} I_1 &= \pi^{3/2} \int_{2/3 - i\infty}^{2/3 + i\infty} \frac{ds}{2\pi i} z^{-s} \left(\frac{2 \csc(\pi s)^3 \sec(\pi s)}{\Gamma(5/2 - s) \Gamma(s - 1)} - \frac{4 \csc(\pi s)^3 \sec(\pi s)}{(s - 2) \Gamma(1 - s) \Gamma(s - 1/2)} \right), \\ I_2 &= \pi^{3/2} \int_{2/3 - i\infty}^{2/3 + i\infty} \frac{ds}{2\pi i} z^{-s} \left(\frac{8 \csc(\pi s)^3 \sec(\pi s)}{\Gamma(3 - s) \Gamma(s - 1/2)} - \frac{2 \csc(\pi s)^3 \sec(\pi s)}{\Gamma(5/2 - s) \Gamma(s)} \right), \\ I_3 &= \pi^{3/2} \int_{2/3 - i\infty}^{2/3 + i\infty} \frac{ds}{2\pi i} z^{-s} \frac{2 \csc(\pi s)^3 \sec(\pi s)}{\Gamma(3/2 - s) \Gamma(s)}. \end{aligned} \quad (2.13)$$

Therefore, after shifting contours and absorb the extra z factors into inverse Mellin transformation, we have that

$$B_1 = 4\pi^{9/2} \left(\frac{2}{3} + 2\sqrt{z} - \frac{4}{\pi^2} f(z)(1+z) \right), \quad (2.14)$$

where the function f is

$$\begin{aligned}
f(z) &= \pi^{7/2} \int_{1/3-i\infty}^{1/3+i\infty} \frac{ds}{2\pi i} z^{-s} \frac{\csc(\pi s)^3 \sec(\pi s)}{\Gamma(1-s)\Gamma(s+1/2)} \\
&= \int_0^\infty \frac{dw}{\sqrt{w(w+z)}} \frac{\log(w)}{w-1} \\
&= \frac{2}{\sqrt{1+z}} \left(\text{Li}_2(1-\tau) - \frac{1}{4} \log(\tau)^2 + \log(\tau-1) \log(\tau) + \frac{\pi^2}{2} \right)
\end{aligned} \tag{2.15}$$

with $\tau = (\sqrt{1+z} + 1)/(\sqrt{1+z} - 1)$, and we use the convolution formula

$$\int_\gamma \frac{ds}{2\pi i} z^{-s} \hat{f}(s) \hat{g}(s) = \int_0^\infty \frac{dw}{w} f(z/w) g(w)$$

to get the first identity in eq.(2.15), where \hat{f} and \hat{g} are Mellin transform of f and g respectively.

Finally, the contribution of all box diagram reads

$$\begin{aligned}
F_{\text{box}} &= \frac{1}{4!} \left(\frac{i}{2\sqrt{\pi}} \right)^4 (3B_1 z^{-1/4} + (z \leftrightarrow z^{-1})) \\
&= \frac{\pi^3}{32} \left(\frac{2}{3} z^{-1/4} + 2z^{1/4} - \frac{4}{\pi^2} z^{-1/4} (1+z) f(z) \right) + (z \leftrightarrow 1/z).
\end{aligned} \tag{2.16}$$

2.3 Ladder diagram

The integrand of ladder diagram is

$$\begin{aligned}
L &= \begin{array}{cccc} 1 & 2 & 3 & 4 \\ \bullet & \circ & \bullet & \circ \end{array} \\
&= 8c^2 \frac{\epsilon_2 \epsilon_3}{D_{1,2} D_{2,3} D_{3,4} s_1 t_2 s_3 t_4} \\
&= -8 \frac{\epsilon(\ell_2, 1, 2, 3, 4) \epsilon(\ell_3, 1, 2, 3, 4)}{(\ell_1 \cdot \ell_2)(\ell_2 \cdot \ell_3)(\ell_3 \cdot \ell_4)(\ell_1 \cdot 2)(\ell_1 \cdot 4)(\ell_2 \cdot 1)(\ell_2 \cdot 3)(\ell_3 \cdot 2)(\ell_3 \cdot 4)(\ell_4 \cdot 1)(\ell_4 \cdot 3)}.
\end{aligned}$$

Here we need to calculate L_1 and L_3 .

For L_3 , we leave ℓ_3 unintegrated, and the ℓ_1 and ℓ_4 -integral is simply the one-loop scale triangle integral, so we get that

$$L_3 = -8\pi^3 \frac{\epsilon(\ell, 1, 2, 3, 4)}{(\ell \cdot 2)(\ell \cdot 4) \sqrt{(\ell \cdot 1)(\ell \cdot 3)(1 \cdot 3)}} \int_2 \frac{\epsilon(\ell_2, 1, 2, 3, 4)}{(\ell_2 \cdot \ell)(\ell_2 \cdot 1)(\ell_2 \cdot 3) \sqrt{(\ell_2 \cdot 2)(\ell_2 \cdot 4)(2 \cdot 4)}}.$$

The ℓ_2 -integral is also a one-loop integral which can be integrated by introducing Feynman parameterization,

$$\int_2 \frac{\epsilon(\ell_2, 1, 2, 3, 4)}{(\ell_2 \cdot \ell)(\ell_2 \cdot 1)(\ell_2 \cdot 3) \sqrt{(\ell_2 \cdot 2)(\ell_2 \cdot 4)(2 \cdot 4)}} = \frac{1}{\sqrt{\pi}} \frac{\epsilon(\ell, 1, 2, 3, 4)}{(2 \cdot 4)(\ell \cdot 1)(\ell \cdot 3)} \int_0^\infty dt \frac{\log(tz)}{\sqrt{t(1+t)}(tz-1)},$$

we introduce the inverse Mellin transformation

$$\frac{\log(tz)}{tz-1} = \pi^2 \int_{1/3-i\infty}^{1/3+i\infty} \frac{ds}{2\pi i} (zt)^{-s} \csc(\pi s)^2,$$

and then perform the t integral, we get that

$$\begin{aligned} & \int_2 \frac{\epsilon(\ell_2, 1, 2, 3, 4)}{(\ell_2 \cdot \ell)(\ell_2 \cdot 1)(\ell_2 \cdot 3) \sqrt{(\ell_2 \cdot 2)(\ell_2 \cdot 4)(2 \cdot 4)}} \\ &= \pi^3 \frac{\epsilon(\ell, 1, 2, 3, 4)}{(2 \cdot 4)(\ell \cdot 1)(\ell \cdot 3)} \int_{1/3-i\infty}^{1/3+i\infty} \frac{ds}{2\pi i} z^{-s} \frac{\csc(\pi s)^3 \sec(\pi s)}{\Gamma(1-s)\Gamma(s+1/2)}. \end{aligned} \quad (2.17)$$

Therefore,

$$\begin{aligned} L_3 &= -8 \frac{\pi^{9/2} \epsilon(\ell, 1, 2, 3, 4)^2}{(\ell \cdot 2)(\ell \cdot 4) \sqrt{(\ell \cdot 1)(\ell \cdot 3)(1 \cdot 3)}} \frac{f(z)/\pi^2}{(2 \cdot 4)(\ell \cdot 1)(\ell \cdot 3)} \\ &= -8 \frac{\pi^{9/2} (1 \cdot 3)(2 \cdot 4)}{(\ell \cdot 2)(\ell \cdot 4) \sqrt{(\ell \cdot 1)(\ell \cdot 3)(1 \cdot 3)}} \frac{(1+z)f(z)}{\pi^2} \\ &= -8\pi^5 \frac{1}{\sqrt{\pi}} \left(\frac{(2 \cdot 4)(1 \cdot 3)}{(\ell \cdot 2)(\ell \cdot 4)(\ell \cdot 1)(\ell \cdot 3)} \right)^{3/4} z^{-1/4} \frac{(1+z)f(z)}{\pi^2}, \end{aligned}$$

where $f(z)$ is a weight-2 polylogarithm introduced in eq.(2.15).

For L_1 , we can first integrate ℓ_2, ℓ_4 , and get a similar integral we meet in the integration of the box diagram,

$$\int_{\ell_2, \ell_4} L = \frac{P_L}{H} + Q_L,$$

where P_L, Q_L are similarly rational functions of scale products and ϵ 's and

$$H = \sqrt{(1 \cdot 3)(\ell_1 \cdot \ell_3)} + \sqrt{(\ell_1 \cdot 3)(\ell_3 \cdot 1)} + \sqrt{(\ell_1 \cdot 1)(\ell_3 \cdot 3)}.$$

Therefore, we follow the same method in the integration of the box diagram, by introducing Mellin transformation for $1/H$, and we get that

$$L_1 = -8\pi^5 \frac{1}{\sqrt{\pi}} \left(\frac{(2 \cdot 4)(1 \cdot 3)}{(\ell \cdot 2)(\ell \cdot 4)(\ell \cdot 1)(\ell \cdot 3)} \right)^{3/4} z^{-1/4} \frac{\log(z/4)^2 + 2\pi^2}{2\pi^2}. \quad (2.18)$$

Therefore,

$$\begin{aligned} F_{\text{ladder}} &= 24 \circ \bullet \circ \bullet = \frac{1}{4!} \left(\frac{i}{2\sqrt{\pi}} \right)^4 (6L_1 + 6L_3 + (z \leftrightarrow z^{-1})) \\ &= -\frac{\pi^3}{8} z^{-1/4} \left(1 + \frac{\log(z/4)^2}{2\pi^2} + \frac{(1+z)f(z)}{\pi^2} \right) + (z \leftrightarrow z^{-1}). \end{aligned} \quad (2.19)$$

3 Cusp anomalous dimension from integrated results

In this section, we extract the cusp anomalous dimension from the functions obtained from the integration of negative geometry. This can be done by integrating out the final loop variable: \mathcal{W}_L diverges and the cusp anomalous dimension is encoded in the coefficient of ϵ^{-2} when the integral is done in $D = 3 - 2\epsilon$.

In [44], it is proposed from the all loop AdS₄/CFT₃ Bethe ansatz that the ABJM cusp anomalous dimension can be obtained from the $\mathcal{N} = 4$ sYM cusp anomalous dimension by simply replacing the interpolating function h^{sYM} to h^{ABJM} :

$$\Gamma_{\text{cusp}}^{\text{ABJM}} = \frac{1}{4} \Gamma_{\text{cusp}}^{\text{sYM}} \Big|_{h^{\text{sYM}} \rightarrow h^{\text{ABJM}}},$$

where the interpolating function for $\mathcal{N} = 4$ sYM is the square root of the coupling [45]

$$h^{\text{sYM}}(\lambda) = \frac{\sqrt{\lambda}}{4\pi}, \quad (3.1)$$

while the interpolating function for ABJM is a complicated function in λ

$$\lambda = \frac{\sinh(2\pi h^{\text{ABJM}})}{2\pi} {}_3F_2 \left(\frac{1}{2}, \frac{1}{2}, \frac{1}{2}; 1, \frac{3}{2}; -\sinh(2\pi h^{\text{ABJM}})^2 \right). \quad (3.2)$$

Therefore, from the weak coupling expansion of $\Gamma_{\text{cusp}}^{\text{sYM}}$ [46]

$$\Gamma_{\text{cusp}}^{\text{sYM}}(h) = 4h^2 - \frac{4}{3}\pi^2 h^4 + \frac{44}{45}\pi^4 h^6 + \dots, \quad (3.3)$$

we get that

$$\Gamma_{\text{cusp}}^{\text{ABJM}}(\lambda) = \lambda^2 - \pi^2 \lambda^4 + \frac{49\pi^4}{30} \lambda^6 + \dots, \quad (3.4)$$

where the leading order at $L = 2$ is checked in [25, 26, 47]. Here we are going to check $\Gamma_{\text{cusp}}^{\text{ABJM}}(\lambda)^{(4)} = -\pi^2$.

To evaluate the last loop integration and extract ϵ^{-2} divergence, one can expand $F_{L-1}(z)$ in z around $z = 0$. This series expansion has logarithmic divergence in general:

$$F_{L-1}(z) = \sum_{p,q} c_{p,q}^{(L-1)} z^p \log(z)^q, \quad (3.5)$$

where q is a non-negative integer, and p can be any rational number. Notice that

$$z^p \log(z)^q = \frac{\partial^q}{\partial p^q} z^p,$$

so we only need to calculate the integral for z^p . As shown in [25, 26], the ϵ^{-2} divergence of the z^p integral in $D = 3 - 2\epsilon$ is simply as

$$\int_{\ell_1} \left(\frac{(1 \cdot 3)(2 \cdot 4)}{(\ell_1 \cdot 1)(\ell_1 \cdot 2)(\ell_1 \cdot 3)(\ell_1 \cdot 4)} \right)^{\frac{3}{4}} z^p = \frac{2}{\sqrt{\pi}} \frac{1}{\Gamma(3/4 - p)\Gamma(3/4 + p)} \epsilon^{-2} + O(\epsilon^{-1}). \quad (3.6)$$

Then, we can replace

$$z^{\pm 1/4} \rightarrow \frac{2}{\pi}, \quad z^{\pm 1/4} \log(z) \rightarrow \mp \frac{4 \log(2)}{\pi}, \quad z^{\pm 1/4} \log(z)^2 \rightarrow -\frac{4\pi}{3} + \frac{8 \log(2)^2}{\pi},$$

and

$$\begin{aligned}
& \frac{1}{\pi^2} z^{-1/4} (1+z) f(z) \\
&= \pi^{3/2} \int_{1/3-i\infty}^{1/3+i\infty} \frac{ds}{2\pi i} (z^{-1/4-s} + z^{3/4-s}) \frac{\csc(\pi s)^3 \sec(\pi s)}{\Gamma(1-s)\Gamma(s+\frac{1}{2})} \\
&\rightarrow 2\pi \int_{1/3-i\infty}^{1/3+i\infty} \frac{ds}{2\pi i} \left(\frac{1}{\Gamma(\frac{1}{2}-s)\Gamma(s+1)} + \frac{1}{\Gamma(\frac{3}{2}-s)\Gamma(s)} \right) \frac{\csc(\pi s)^3 \sec(\pi s)}{\Gamma(1-s)\Gamma(s+\frac{1}{2})} \\
&= \frac{2}{\pi} \int_{1/3-i\infty}^{1/3+i\infty} \frac{ds}{2\pi i} \frac{\csc(\pi s)^2}{(1-2s)s} \\
&= \frac{4}{3\pi}
\end{aligned}$$

in F_{star} , F_{ladder} and F_{box} to get the corresponding contribution to the 4-loop cusp anomalous dimension $\Gamma_{\text{cusp}}^{(4)}$:

$$F_{\text{star}} = -\frac{\pi^3}{12} (z^{-1/4} + z^{1/4}) \rightarrow -\frac{\pi^2}{3}, \quad (3.7)$$

$$\begin{aligned}
F_{\text{ladder}} &= -\frac{\pi^3}{8} z^{-1/4} \left(1 + \frac{\log(z/4)^2}{2\pi^2} + \frac{(1+z)f(z)}{\pi^2} \right) + (z \leftrightarrow z^{-1}) \\
&\rightarrow 2 \times \frac{\pi^3}{8} \left(-\frac{2}{\pi} + \frac{2}{3\pi} - \frac{4}{3\pi} \right) = -\frac{2\pi^2}{3}.
\end{aligned} \quad (3.8)$$

but the box does not contribute the Γ_{cusp}

$$\begin{aligned}
F_{\text{box}} &= \frac{\pi^3}{32} \left(\frac{7}{3} (z^{-1/4} + z^{1/4}) - \frac{4}{\pi^2} z^{-1/4} (1+z) f(z) - \frac{4}{\pi^2} z^{1/4} (1+1/z) f(1/z) \right) \\
&\rightarrow 2 \times \frac{\pi^3}{32} \left(\frac{8}{3\pi} - 4 \frac{4}{3\pi} \right) = 0.
\end{aligned} \quad (3.9)$$

Therefore, 4-loop cusp anomalous dimension is

$$\Gamma_{\text{cusp}}^{(4)} = -\frac{\pi^2}{3} - \frac{2\pi^2}{3} = -\pi^2, \quad (3.10)$$

which agrees with eq.(3.4) at $L = 4$.

Note that the box diagram does not contribute to Γ_{cusp} , which means that if we integrate all loop momenta in the box diagram, we have that

$$\int \prod_{i=1}^4 d^3 \ell_i \quad \begin{array}{c} \bullet \quad 4 \\ \circ \quad \quad \circ \\ | \quad \quad | \\ \bullet \quad 1 \quad \bullet \quad 2 \\ \circ \quad \quad \circ \end{array} = O(\epsilon^{-1}). \quad (3.11)$$

If we go back to eq.(1.16), the integrand of the box diagram can be decomposed into three parts with 0, 2 and 4 ϵ_i 's on its numerator as $B = N_0 + N_2 + N_4$, and we find that

$$\int \prod_{i=1}^4 d^3 \ell_i N_4 = -\int \prod_{i=1}^4 d^3 \ell_i N_2 \propto \log(2)\epsilon^{-2} + O(\epsilon^{-1}), \quad \int \prod_{i=1}^4 d^3 \ell_i N_0 = O(\epsilon^{-1}).$$

Therefore, it is so non-trivial that the construction of the integrand of the box diagram weakens the IR divergence. It will be interesting to see this directly from the integrand. The IR divergence of the Feynman integral in $\mathcal{N} = 4$ sYM appears when one of the loop momentum goes to a collinear region [2, 17]

$$\ell_i \rightarrow ax_k + (1 - a)x_{k+1} + \eta k_i \quad (3.12)$$

for $k = 1, \dots, 4$, where a is a parameter, k_i is a reference momentum and η is a small positive number. In [17], it is argued that if one loop momentum is in a collinear region, then the condition eq.(1.9) requires that all loop momentua are in the same collinear region, which weakens the divergence of a L -loop integral to a one-loop divergence $O(\epsilon^{-2})$. Since there are further constrains on negative geometries of ABJM theory [13], it would be possible that the divergence could be further weakened for some negative geometries. We leave this for further work.

4 Higher loop ladders

In this section, we consider a special kind of all-loop negative geometries corresponding to ladder diagrams.

Integrands of ladder diagrams have a recursive structure [13]

$$\begin{array}{cccccccccccc} \bullet & \circ & \bullet & \circ & \bullet & \dots & \dots & \dots & \bullet & \circ \\ 1 & 2 & 3 & 4 & 5 & \dots & \dots & \dots & n & n+1 \end{array} = \begin{array}{cccccccccccc} \bullet & \circ & \bullet & \circ & \bullet & \dots & \dots & \dots & \bullet \\ 1 & 2 & 3 & 4 & 5 & \dots & \dots & \dots & n \end{array} \times \frac{2\epsilon_n}{D_{n,n+1}t_{n+1}}$$

and the initial ladder is

$$\begin{array}{cc} \bullet & \circ \\ 1 & 2 \end{array} = \frac{2c^2}{s_1 t_2 D_{12}}.$$

For these two ladder L_{n+1} and L_n , if we already have the integral of L_n with only ℓ_n unintegrated

$$\int_{1, \dots, n-1} L_n = \alpha_{\text{black}}(\ell_n) \tilde{L}_n(z_n),$$

where $\alpha_{\text{black}}(\ell_n)$ is a non-DCI prefactor which makes \tilde{L}_n be the function in z_n . The prefactor is universal for nodes with the same color, and α_{white} is given by interchanging dual points $X_1 \leftrightarrow X_2, X_3 \leftrightarrow X_4$ in α_{black} . Following the prefactor eq.(2.11) used in the calculating of box diagram, we choose

$$\alpha_{\text{black}}(\ell) = \frac{(2 \cdot 4) \sqrt{(1 \cdot 3)}}{(\ell \cdot 2)(\ell \cdot 4) \sqrt{(\ell \cdot 1)(\ell \cdot 3)}}, \quad \alpha_{\text{white}}(\ell) = \frac{(1 \cdot 3) \sqrt{(2 \cdot 4)}}{(\ell \cdot 1)(\ell \cdot 3) \sqrt{(\ell \cdot 2)(\ell \cdot 4)}}, \quad (4.1)$$

so $\tilde{L}_2 = 2\pi^{3/2}$. Therefore, the recursion relation becomes

$$\alpha_{\text{white}}(\ell_{n+1}) \tilde{L}_{n+1}(z_{n+1}) = \int_{1, \dots, n} L_{n+1} = \int_n \frac{2\epsilon_n}{D_{n,n+1}t_{n+1}} \alpha_{\text{black}}(\ell_n) \tilde{L}_n(z_n) \quad (4.2)$$

and the similar formula for ladders with the inverse color.

We can see eq.(4.2) as an integral transformation of $\hat{L}_n(z_n)$ in ℓ_n -space with the kernel

$$\frac{2\epsilon_n}{D_{n,n+1}t_{n+1}}\alpha_{\text{black}}(\ell_n) = \frac{2}{(\ell_{n+1}\cdot 1)(\ell_{n+1}\cdot 3)} \frac{\epsilon(1, 2, 3, 4, \ell_n)}{(\ell_n\cdot \ell_{n+1})(\ell_n\cdot 2)(\ell_n\cdot 4)\sqrt{(\ell_n\cdot 1)(\ell_n\cdot 3)}}.$$

To perform the loop integral, we can further choose a Mellin representation $\tilde{L}_n(z_n)$ as

$$\tilde{L}_n(z_n) = \int_{\gamma} \frac{ds}{2\pi i} \hat{L}_n(s) z_n^{-s},$$

then the recursion relation becomes a new integral transformation in the Mellin s -space with the kernel

$$K(s) = \int_n \frac{\epsilon(1, 2, 3, 4, \ell_n)}{(\ell_n\cdot \ell_{n+1})(\ell_n\cdot 2)(\ell_n\cdot 4)\sqrt{(\ell_n\cdot 1)(\ell_n\cdot 3)}} z_n^{-s},$$

and we can first integrate ℓ_n in this kernel. From the definition of z_n eq.(1.19), $K(s)$ is a one-loop integral of the form eq.(A.1), and its Mellin representation is given in the Appendix:

$$K(s) = \int_{\gamma} \frac{dt}{2\pi i} z_{n+1}^{-t} \frac{\sqrt{\pi} \csc(\pi t)^2 \Gamma(s-t) \Gamma(-s+t+\frac{1}{2})}{\Gamma(\frac{1}{2}-s)^2 \Gamma(s+1)^2} \frac{(1\cdot 3)(2\cdot 4)\epsilon(1, 2, 3, 4, \ell_{n+1})}{(\ell_{n+1}\cdot 1)(\ell_{n+1}\cdot 3)(\ell_{n+1}\cdot 2)(\ell_{n+1}\cdot 4)}.$$

Therefore, we get the recursion relation in Mellin space

$$\frac{1}{\sqrt{1+z^{-1}}} \tilde{L}_{n+1}(z) = 2\sqrt{\pi} \int_{\gamma_s, \gamma_t} \frac{ds dt}{(2\pi i)^2} z^{-t} \frac{\csc(\pi t)^2 \Gamma(-s+t+1/2) \Gamma(-t+s)}{\Gamma(1+s)^2 \Gamma(1/2-s)^2} \hat{L}_n(s), \quad (4.3)$$

and the contour is chosen such that

$$\text{Re}[-s+t+1/2] > 0, \quad \text{Re}[-t+s] > 0, \quad -1 < \text{Re}[t] < 0.$$

Similarly the further recursion to $\tilde{L}_{n+2}(z)$ is in the invert color, so it is given by replacing $z \rightarrow z^{-1}$ (and correspondingly $s, t \rightarrow -s, -t$) in eq.(4.3):

$$\frac{1}{\sqrt{1+z}} \tilde{L}_{n+2}(z) = 2\sqrt{\pi} \int_{\gamma_s, \gamma_t} \frac{ds dt}{(2\pi i)^2} z^{-t} \frac{\csc(\pi t)^2 \Gamma(s-t+1/2) \Gamma(t-s)}{\Gamma(1-s)^2 \Gamma(1/2+s)^2} \hat{L}_{n+1}(s). \quad (4.4)$$

As an example, we first consider the following integral

$$\begin{array}{c} 1 \\ \circ - \bullet \end{array} = \frac{2c^2}{t_1 s_2 D_{12}}, \quad \begin{array}{c} 1 \quad 2 \quad 3 \\ \circ - \bullet - \circ \end{array} = \frac{4c^2 \epsilon_2}{t_1 s_2 t_3 D_{12} D_{23}}.$$

It is easy to perform L_2 by using the one-loop scale triangle:

$$\tilde{L}_2(z) = 2\pi^{3/2} \quad \text{or} \quad \hat{L}_2(s) = 2\pi^{3/2} 2\pi i \delta(s), \quad (4.5)$$

therefore from eq.(4.3)

$$\frac{1}{\sqrt{1+z^{-1}}} \tilde{L}_3(z) = 2\pi^3 \int_{-1/4-i\infty}^{-1/4+i\infty} \frac{dt}{2\pi i} z^{-t} \frac{\csc(\pi t)^3 \sec(\pi t)}{\Gamma(1/2-t)\Gamma(1+t)} = \frac{2}{\sqrt{\pi}} f(1/z),$$

where the function $f(z)$ is defined in eq.(2.15), so \tilde{L}_3 is a pure weight-2 polylogarithm

$$\tilde{L}_3(z) = \frac{4}{\sqrt{\pi}} \left(\text{Li}_2(1-x) - \frac{1}{4} \log(x)^2 + \log(x-1) \log(x) + \frac{\pi^2}{2} \right) \quad (4.6)$$

with $x = (\sqrt{1+z^{-1}}+1)/(\sqrt{1+z^{-1}}-1)$, which is first evaluated in [25, 26], and its symbol alphabet is $\{x, 1-x\}$.

Similarly, we can calculate \tilde{L}_5 from $\tilde{L}_4(z)$ by eq.(4.3). The Mellin transformation of $\log(z/4)^2 + 2\pi^2$ is

$$\hat{L}_4(s) \propto 2\pi^2 + (\partial_s - \log(4))^2 2\pi i \delta(s),$$

so after a little simplification and using the convolution formula

$$\int_{\gamma} \frac{ds}{2\pi i} z^{-s} \hat{f}(s) \hat{g}(s) = \int_0^{\infty} \frac{dw}{w} f(z/w) g(w),$$

we get that

$$\frac{1}{\sqrt{1+z^{-1}}} \tilde{L}_5(z) \propto \int_0^{\infty} \frac{z dw}{\sqrt{w(w+1)}(w-z)} \log\left(\frac{z}{w}\right) \left(\log(4w)^2 + \frac{2\pi^2}{3} \right). \quad (4.7)$$

By replacing $w = (1-y)^2/(4y)$ and $z = (1-x)^2/(4x)$, the integral becomes

$$\tilde{L}_5(z) \propto \int_{0 < y < 1} d \log\left(\frac{1-xy}{y-x}\right) \log\left(\frac{(x-1)^2 y}{x(y-1)^2}\right) \left(\log\left(\frac{(1-y)^2}{y}\right)^2 + \frac{2\pi^2}{3} \right),$$

which is a standard iterated integral of polylogarithms, and it has the same symbol alphabet as $\tilde{L}_3(z)$. We list the function of this integral in the Appendix.

The calculation of $\tilde{L}_4(z)$ from recursion relation is quite tricky. We want to derive it from $\tilde{L}_2(z) \propto 1$ by first apply eq.(4.3) and then eq.(4.4). However, we already know that

$$\tilde{L}_4(z) \propto \log(z/4)^2 + 2\pi^2$$

is a polynomial of $\log(z/4)$ from the concrete calculation in section 2.3. We find it is only possible to first take the residue around $-s+t+1/2=0$ in eq.(4.4), and $z^{-t} \rightarrow z^{-s+1/2}$ which produce an extra \sqrt{z} to cancel the a \sqrt{z} from $\sqrt{1+1/z}$ in eq.(4.3), and then we need to take the residue around $s=0$ in eq.(4.4) since other pole will produce a power of z . After taking above residues and removing irrelevant factors, we re-obtain that

$$\tilde{L}_4(z) \propto \oint_{t=0} \frac{dt}{2\pi i} z^{-t} \frac{4\sqrt{\pi} \csc(2\pi t)^2}{t \Gamma(1-t) \Gamma(t+1/2)} \propto \log(z/4)^2 + 2\pi^2$$

through this rough reasoning.

Similarly, for the recursion from even loop ladder $\tilde{L}_{2n}(z)$ to $\tilde{L}_{2n+2}(z)$, we conjecture that if there is a term

$$\log(z)^k = \left. \frac{\partial^k}{\partial p^k} z^p \right|_{p=0}$$

in the $\tilde{L}_{2n}(z)$, it will produce a term

$$T[\log(z)^k] = -4\pi^{3/2} \oint_{t=0} \frac{dt}{2\pi i} z^{-t} \frac{\partial^k}{\partial p^k} \frac{\csc(2\pi t)^2 \Gamma(p+t+1/2) \Gamma(-t-p)}{\Gamma(1-p)^2 \Gamma(p+1/2)^2 \Gamma(1/2+t)^2 \Gamma(1-t)^2} \Big|_{p=0} \quad (4.8)$$

in the $\tilde{L}_{2n+2}(z)$. Since $\tilde{L}_{2n}(z)$ would be a function in $\log(z/4)$, it is also convenient to use the variant

$$T[\log(z/4)^k] = -4\pi^{3/2} \oint_{t=0} \frac{dt}{2\pi i} z^{-t} \frac{\partial^k}{\partial p^k} \frac{4^{-p} \csc(2\pi t)^2 \Gamma(p+t+1/2) \Gamma(-t-p)}{\Gamma(1-p)^2 \Gamma(p+1/2)^2 \Gamma(1/2+t)^2 \Gamma(1-t)^2} \Big|_{p=0} \quad (4.9)$$

The integral has a closed formula:

$$T[\log(z/4)^k] = \frac{\log(z/4)^{k+2}}{\pi^2(k+1)(k+2)} + B_k \log(z/4) + C_k$$

with

$$B_k = \frac{1}{(k+1)(k+2)} \frac{\partial^{k+2}}{\partial p^{k+2}} \frac{4^{-p}}{\pi^{3/2} \Gamma(-p) \Gamma(p+1/2)} \Big|_{p=0},$$

$$C_k = -\frac{1}{(k+1)(k+2)} \frac{\partial^{k+2}}{\partial p^{k+2}} \frac{4^{-p}(-\psi(-p) + \psi(p+1/2) + \log(4))}{\pi^{3/2} \Gamma(-p) \Gamma(p+1/2)} \Big|_{p=0},$$

where $\psi(z) = \frac{d}{dz} \log(\Gamma(z))$ is the digamma function.

Therefore, from $\tilde{L}_4 \propto \log(z/4)^2 + 2\pi^2$, our conjecture predicts that

$$\tilde{L}_6 = T[\tilde{L}_4] \propto -4\zeta_3 \log\left(\frac{z}{4}\right) + \frac{1}{12} \log\left(\frac{z}{4}\right)^4 + \pi^2 \log\left(\frac{z}{4}\right)^2 + \frac{17\pi^4}{9}, \quad (4.10)$$

$$\tilde{L}_8 = T[\tilde{L}_6] \propto -\frac{2}{3} \zeta_3 \log\left(\frac{z}{4}\right)^3 - 4\pi^2 \zeta_3 \log\left(\frac{z}{4}\right) - 12\zeta_5 \log\left(\frac{z}{4}\right) + 4\zeta_3^2 + \frac{1}{360} \log\left(\frac{z}{4}\right)^6 + \frac{1}{12} \pi^2 \log\left(\frac{z}{4}\right)^4 + \frac{17}{18} \pi^4 \log\left(\frac{z}{4}\right)^2 + \frac{49\pi^6}{27} \quad (4.11)$$

and so on. Note that since

$$\pi^2(z\partial_z)^2 T[\log(z/4)^k] = \log(z/4)^k,$$

we have a differential equation to relate \tilde{L}_{2n} with \tilde{L}_{2n+2} :

$$\pi^2(z\partial_z)^2 \tilde{L}_{2n+2} = \tilde{L}_{2n}. \quad (4.12)$$

It is also easy to compute the cusp anomalous dimension contribution from conjectured \tilde{L}_6 , \tilde{L}_8 and \tilde{L}_{10} , and we find that they are proportional to π^4 , π^6 and π^8 . Therefore, although there are zeta values like ζ_3, ζ_5 in \tilde{L}_{2n+2} , they do not contribute to the cusp anomalous dimension at $L = 2, 4, 6, 8, 10$. It is natural to further conjecture that it will hold for any $2n$ -loop.

The computation of cusp anomalous dimension will also provide a non-trivial check for our conjecture. For example, we can compute the 8-loop ladder with the node 5

unintegrated (suppose that the node 5 is black), then it becomes the product of two ladders with length 4 and 5, and

$$\int_{1,2,3,4} \int_{6,7,8} L_8 \propto (z^{1/4} + z^{-1/4}) \tilde{L}_4 \frac{\tilde{L}_5}{\sqrt{1+z^{-1}}}, \quad (4.13)$$

and its contribution to cusp anomalous dimension should equal to the contribution from \tilde{L}_8 since they are the same leading divergence of ϵ^{-2} of

$$\int_{1,2,3,4,5,6,7,8} L_8.$$

5 Discussions

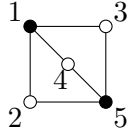
In this note, we have integrated the ABJM negative geometries at $L = 4$ and ladder-type negative geometries at all loop by recursion relation, both based on introducing suitable Mellin transformation.

One of most interesting result at $L = 4$ is that the box diagram

$$\int \prod_{i=1}^4 d^3 \ell_i \quad \begin{array}{ccc} & 4 & 3 \\ & \circ & \bullet \\ | & & | \\ \bullet & & \circ \\ 1 & & 2 \end{array} = O(\epsilon^{-1})$$

is less divergent than other negative geometry at $L = 4$. It will be interesting to see that directly from its negative geometry structure, which can be generalized to more complicated diagrams. As inspired by this diagram, we can make a wild conjecture that even for higher loop negative geometry, any bipartite diagram with loops would diverge as ϵ^{-1} (or even ϵ^0). Since when the number of loop momenta is odd, the integration of negative geometry diverges as ϵ^{-1} [25, 26]. Therefore, the next non-trivial check will be at $L = 6$, where we have already seen that the integration of $L = 6$ ladder has the ϵ^{-2} divergence. If we are lucky enough that the conjecture was correct, we only need to consider the tree bipartite diagrams of negative geometries when computing the cusp anomalous dimension.

Although the negative geometry with an odd number of loop momenta do not contribute the cusp anomalous dimension, it is still interesting to integrate it at $L = 5$. The first integrated 5-loop negative geometry is the ladder \tilde{L}_5 eq.(4.7), while the most complicated negative geometry would correspond to a bipartite graph with two loops



with the integrand

$$\begin{aligned} T_6 = & \frac{4}{cs_1 t_2 t_3 t_4 s_5 D_{1,2} D_{1,3} D_{1,4} D_{2,5} D_{3,5} D_{4,5}} (-8\epsilon_1 \epsilon_2 \epsilon_3 \epsilon_4 \epsilon_5 N_{15}^s + c\epsilon_2 \epsilon_3 \epsilon_4 P_a \\ & + c[\epsilon_1 \epsilon_2 \epsilon_3 P_b + (\ell_1 \leftrightarrow \ell_5) + \epsilon_1 \epsilon_2 \epsilon_5 P_c + \text{cyc}(\ell_2, \ell_3, \ell_4)] \\ & + c^2[\epsilon_1 P_d + (\ell_1 \leftrightarrow \ell_5)] + c^2[\epsilon_2 P_e + \text{cyc}(\ell_2, \ell_3, \ell_4)]), \end{aligned}$$

which is first computed in [13], where

$$\begin{aligned}
P_a &:= -20s_1s_5 + 16t_1t_5 + (N_{15}^s)^2, & P_b &:= 6s_5N_{14}^s, & P_c &:= N_{15}^sN_{34}^t - 4N_{1,3,5,4}^{\text{cyc}}, \\
P_d &:= -s_5(N_{12}^sN_{34}^t + \text{cyc}(\ell_2, \ell_3, \ell_4)) + [2\langle \ell_512 \rangle^2 \langle \ell_112 \rangle \langle \ell_234 \rangle \langle \ell_334 \rangle \langle \ell_434 \rangle + \text{cyc}(1, 2, 3, 4)] \\
&\quad + 2t_5[\langle \ell_114 \rangle (\langle \ell_214 \rangle \langle \ell_323 \rangle \langle \ell_423 \rangle + \text{cyc}(\ell_2, \ell_3, \ell_4)) + (14 \leftrightarrow 23)], \\
P_e &:= 2s_1s_5(N_{34}^t - N_{34}^s) - 4t_1t_5N_{34}^t - [s_5(\langle \ell_112 \rangle^2 \langle \ell_334 \rangle \langle \ell_434 \rangle + (12 \leftrightarrow 34)) + (\ell_1 \leftrightarrow \ell_5)] \\
&\quad + N_{15}^s(\langle \ell_114 \rangle \langle \ell_514 \rangle \langle \ell_323 \rangle \langle \ell_423 \rangle + (14 \leftrightarrow 23)).
\end{aligned}$$

It is important to look for a nice way to integrate negative geometries starting at $L = 5$, it seems that both canonical differential equations [48] and Mellin transformation used in this note will become not processable. The most natural way is directly integrating it in momentum twistor space where we still do not understand how to take the contour. Since we only need look for 3 contours for each 3D loop momentum, the ABJM theory will be a nice playground to test it.

For ladder diagrams we consider in this note, we provide a conjecture of recursion relation from \tilde{L}_{2n} to \tilde{L}_{2n+2} , and we also conjecture that they only contribute power of π to the cusp anomalous dimension while there are other zeta values in their functions. Since some derivation is not so rigorous, we need more checks for these conjectures. One possible check is to integrate the loop momenta in different orders, which gives the same leading divergence of ϵ^{-2} .

Despite the correctness of conjectures, it is interesting to resum these ladders. According to the differential equation eq.(4.12) for $n \geq 1$

$$\pi^2(z\partial_z)^2\tilde{L}_{2n+2} = \tilde{L}_{2n},$$

we can define $K(\lambda, z) = \sum_{n=1}^{\infty} \lambda^{2n} \tilde{L}_{2n}$, then there is a differential equation for resummed $K(\lambda, z)$

$$(z\partial_z)^2K(\lambda, z) = \frac{\lambda^2}{\pi^2}K(\lambda, z),$$

the solution is

$$K(\lambda, z) = c_1(\lambda) \sinh\left(\frac{\lambda}{\pi} \log\left(\frac{z}{4}\right)\right) + c_2(\lambda) \cosh\left(\frac{\lambda}{\pi} \log\left(\frac{z}{4}\right)\right) \quad (5.1)$$

depending on two unknown functions $c_1(\lambda)$ and $c_2(\lambda)$. We leave it to further work.

Acknowledgement

Zhenjie Li thanks Song He, Chia-Kai Kuo, Yichao Tang, Qinglin Yang, Yao-Qi Zhang for stimulating discussions and collaborations on related projects, and thanks Bernhard Mistlberger for discussion about the numerical evaluating the 3D Feynman integral. We are grateful to Martin Lagares and Shun-Qing Zhang for sharing their results with us. This work is supported in part by the U.S. Department of Energy under contract number DE-AC02-76SF00515.

Note added: While this work was in progress, we were made aware of an upcoming work [48], where the finite function up to $L = 4$ has been computed and the two results agree.

A Collection of useful 1-loop integrals

We need two 1-loop integrals in this note

$$I_1 = \int_{\ell} \frac{1}{(\ell \cdot 1)^{q_1} (\ell \cdot 2)^{q_2} (\ell \cdot 3)^{q_3} (\ell \cdot 4)^{q_4} (\ell \cdot \ell')^{q_5}} \quad (\text{A.1})$$

with $q_1 + \dots + q_5 = 3$ and

$$I_2 = \int_{\ell} \frac{N[\ell]}{(\ell \cdot 1)^{q_1} (\ell \cdot 2)^{q_2} (\ell \cdot 3)^{q_3} (\ell \cdot 4)^{q_4} (\ell \cdot \ell')^{q_5}} \quad (\text{A.2})$$

with $q_1 + \dots + q_5 = 4$, where $N[\ell]$ is linear in dual momentum ℓ and $N[1] = N[3] = 0$, for example, $N[\ell]$ could be ϵ_{ℓ} or $(\ell \cdot 2)$ or $(\ell \cdot 4)$.

Two special cases is scale triangle

$$\int_{\ell} \frac{1}{(\ell \cdot a)(\ell \cdot b)(\ell \cdot c)} = \frac{\pi^{3/2}}{\sqrt{(a \cdot b)(b \cdot c)(c \cdot a)}}$$

and the box integral with a numerator $N[\ell]$,

$$\int_{\ell} \frac{N[\ell]}{(\ell \cdot \ell_1)(\ell \cdot \ell_3)(\ell \cdot 1)(\ell \cdot 3)} = \pi^{3/2} \frac{N[\ell_1]/\sqrt{(\ell_1 \cdot 1)(\ell_1 \cdot 3)} + N[\ell_3]/\sqrt{(\ell_3 \cdot 1)(\ell_3 \cdot 3)}}{\sqrt{(1 \cdot 3)(\ell_1 \cdot \ell_3)} + \sqrt{(\ell_1 \cdot 3)(\ell_3 \cdot 1)} + \sqrt{(\ell_1 \cdot 1)(\ell_3 \cdot 3)}}.$$

The most general cases can be done by introducing Feynman parameterization,

$$A = a_5 \ell' + \sum_{i=1}^4 a_i X_i,$$

then for I_1

$$\frac{1}{(\ell \cdot 1)^{q_1} (\ell \cdot 2)^{q_2} (\ell \cdot 3)^{q_3} (\ell \cdot 4)^{q_4} (\ell \cdot \ell')^{q_5}} = \int \frac{d^5 a}{\text{GL}(1)} \frac{\Gamma(3)}{(\ell \cdot A)^3} \prod_i \frac{a_i^{q_i-1}}{\Gamma(q_i)}$$

and for I_2

$$\frac{N[\ell]}{(\ell \cdot 1)^{q_1} (\ell \cdot 2)^{q_2} (\ell \cdot 3)^{q_3} (\ell \cdot 4)^{q_4} (\ell \cdot \ell')^{q_5}} = - \int \frac{d^5 a}{\text{GL}(1)} \frac{\Gamma(3) N[\partial A]}{(\ell \cdot A)^3} \prod_i \frac{a_i^{q_i-1}}{\Gamma(q_i)},$$

where the loop integral becomes trivial, and after integrating ℓ and Feynman parameters a_1, a_2 and a_5 , we get that

$$I_1 = (1 \cdot 3)^{-q_1 - q_2 - q_3 + \frac{3}{2}} (2 \cdot 4)^{-q_4} (\ell' \cdot 1)^{q_2 + q_3 - \frac{3}{2}} (\ell' \cdot 2)^{q_4 - q_2} (\ell' \cdot 3)^{q_1 + q_2 - \frac{3}{2}} \frac{\Gamma(-q_1 - q_2 + 3/2)}{\pi^{3/2} \Gamma(q_3) \Gamma(-q_1 - q_2 - q_3 - q_4 + 3) \Gamma(q_4)} \int_{\mathbb{R}_+^2} da_3 da_4 a_3^{q_3-1} (a_3 + 1)^{-q_1} a_4^{q_4-1} (a_4 + 1)^{-q_2} (a_4 z' + a_3)^{q_1 + q_2 - \frac{3}{2}} \quad (\text{A.3})$$

and

$$I_2 = (1 \cdot 3)^{-q_1 - q_2 - q_3 + \frac{5}{2}} (2 \cdot 4)^{-q_4} (\ell' \cdot 1)^{q_2 + q_3 - \frac{5}{2}} (\ell' \cdot 2)^{q_4 - q_2} (\ell' \cdot 3)^{q_1 + q_2 - \frac{5}{2}} \frac{\Gamma(-q_1 - q_2 + 5/2) N[\ell']}{\pi^{3/2} \Gamma(q_3) \Gamma(-q_1 - q_2 - q_3 - q_4 + 4) \Gamma(q_4)} \int_{\mathbb{R}_+^2} da_3 da_4 a_3^{q_3 - 1} (a_3 + 1)^{-q_1} a_4^{q_4 - 1} (a_4 + 1)^{-q_2} (a_4 z' + a_3)^{q_1 + q_2 - \frac{5}{2}}. \quad (\text{A.4})$$

The a_3, a_4 -integral can be further integrated if we introduce the Mellin transform of $(a_4 z' + z_3)^k$

$$(a_4 z' + z_3)^k = \int_{\gamma} \frac{ds}{2\pi i} (z')^{-s} a_4^{-s} a_3^{k+s} \frac{\Gamma(s) \Gamma(-k-s)}{\Gamma(-k)},$$

and we get that

$$I_1 = (1 \cdot 3)^{-q_1 - q_2 - q_3 + \frac{3}{2}} (2 \cdot 4)^{-q_4} (\ell' \cdot 1)^{q_2 + q_3 - \frac{3}{2}} (\ell' \cdot 2)^{q_4 - q_2} (\ell' \cdot 3)^{q_1 + q_2 - \frac{3}{2}} \int_{\gamma} \frac{ds}{2\pi i} (z')^{-s} \frac{\Gamma(s) \Gamma(-s - q_1 - q_2 + \frac{3}{2}) \Gamma(-s - q_2 - q_3 + \frac{3}{2}) \Gamma(s + q_1 + q_2 + q_3 - \frac{3}{2}) \Gamma(s + q_2 - q_4) \Gamma(q_4 - s)}{\pi^{3/2} \Gamma(q_1) \Gamma(q_2) \Gamma(q_3) \Gamma(-q_1 - q_2 - q_3 - q_4 + 3) \Gamma(q_4)},$$

and

$$I_2 = (1 \cdot 3)^{-q_1 - q_2 - q_3 + \frac{5}{2}} (2 \cdot 4)^{-q_4} (\ell' \cdot 1)^{q_2 + q_3 - \frac{5}{2}} (\ell' \cdot 2)^{q_4 - q_2} (\ell' \cdot 3)^{q_1 + q_2 - \frac{5}{2}} N[\ell'] \int_{\gamma} \frac{ds}{2\pi i} (z')^{-s} \frac{\Gamma(s) \Gamma(-s - q_1 - q_2 + \frac{5}{2}) \Gamma(-s - q_2 - q_3 + \frac{5}{2}) \Gamma(s + q_1 + q_2 + q_3 - \frac{5}{2}) \Gamma(s + q_2 - q_4) \Gamma(q_4 - s)}{\pi^{3/2} \Gamma(q_1) \Gamma(q_2) \Gamma(q_3) \Gamma(-q_1 - q_2 - q_3 - q_4 + 4) \Gamma(q_4)}.$$

B Function of 5-loop ladder

Let $z = (1-x)^2/(4x)$, the 5-loop ladder is given by the integral

$$\tilde{L}_5(z) \propto \int_{0 < y < 1} d \log \left(\frac{1-xy}{y-x} \right) \log \left(\frac{(x-1)^2 y}{x(y-1)^2} \right) \left(\log \left(\frac{(1-y)^2}{y} \right)^2 + \frac{2\pi^2}{3} \right),$$

and the result of this integral in generalized polylogarithms is

$$\begin{aligned} & \frac{2}{3} \pi^2 G(x^{-1}, 0; 1) - \frac{4}{3} \pi^2 G(x^{-1}, 1; 1) - \frac{2}{3} \pi^2 G(x, 0; 1) + \frac{4}{3} \pi^2 G(x, 1; 1) + 6G(x^{-1}, 0, 0, 0; 1) - \\ & 12G(x^{-1}, 0, 0, 1; 1) - 12G(x^{-1}, 0, 1, 0; 1) + 24G(x^{-1}, 0, 1, 1; 1) - 12G(x^{-1}, 1, 0, 0; 1) + \\ & 24G(x^{-1}, 1, 0, 1; 1) + 24G(x^{-1}, 1, 1, 0; 1) - 48G(x^{-1}, 1, 1, 1; 1) - 6G(x, 0, 0, 0; 1) + \\ & 12G(x, 0, 0, 1; 1) + 12G(x, 0, 1, 0; 1) - 24G(x, 0, 1, 1; 1) + 12G(x, 1, 0, 0; 1) - \\ & 24G(x, 1, 0, 1; 1) - 24G(x, 1, 1, 0; 1) + 48G(x, 1, 1, 1; 1) + \log(x + x^{-1} - 2) \times \\ & \left(2G(x^{-1}, 0, 0; 1) - 4G(x^{-1}, 0, 1; 1) - 4G(x^{-1}, 1, 0; 1) + 8G(x^{-1}, 1, 1; 1) - 2G(x, 0, 0; 1) + \right. \\ & \left. 4G(x, 0, 1; 1) + 4G(x, 1, 0; 1) - 8G(x, 1, 1; 1) + \frac{2}{3} \pi^2 \log(1-x) - \frac{2}{3} \pi^2 \log(1-x^{-1}) \right), \end{aligned}$$

and its symbol equals

$$16[1-x, x, 1-x, 1-x] - 8[1-x, x, 1-x, x] - 8[1-x, x, x, 1-x] + \\ 4[1-x, x, x, x] - 8[x, x, 1-x, 1-x] + 4[x, x, 1-x, x] + 4[x, x, x, 1-x] - 2[x, x, x, x],$$

where we use $[a, b, c, d]$ to represent $a \otimes b \otimes c \otimes d$.

References

- [1] N. Arkani-Hamed and J. Trnka, “The Amplituhedron,” *JHEP* **10** (2014) 030, [arXiv:1312.2007 \[hep-th\]](#).
- [2] N. Arkani-Hamed and J. Trnka, “Into the Amplituhedron,” *JHEP* **12** (2014) 182, [arXiv:1312.7878 \[hep-th\]](#).
- [3] N. Arkani-Hamed, H. Thomas, and J. Trnka, “Unwinding the Amplituhedron in Binary,” *JHEP* **01** (2018) 016, [arXiv:1704.05069 \[hep-th\]](#).
- [4] N. Arkani-Hamed, Y. Bai, and T. Lam, “Positive Geometries and Canonical Forms,” *JHEP* **11** (2017) 039, [arXiv:1703.04541 \[hep-th\]](#).
- [5] N. Arkani-Hamed, P. Benincasa, and A. Postnikov, “Cosmological Polytopes and the Wavefunction of the Universe,” [arXiv:1709.02813 \[hep-th\]](#).
- [6] N. Arkani-Hamed, Y. Bai, S. He, and G. Yan, “Scattering Forms and the Positive Geometry of Kinematics, Color and the Worldsheet,” *JHEP* **05** (2018) 096, [arXiv:1711.09102 \[hep-th\]](#).
- [7] N. Arkani-Hamed, S. He, and T. Lam, “Stringy canonical forms,” *JHEP* **02** (2021) 069, [arXiv:1912.08707 \[hep-th\]](#).
- [8] N. Arkani-Hamed, S. He, G. Salvatori, and H. Thomas, “Causal Diamonds, Cluster Polytopes and Scattering Amplitudes,” [arXiv:1912.12948 \[hep-th\]](#).
- [9] N. Arkani-Hamed, S. He, T. Lam, and H. Thomas, “Binary Geometries, Generalized Particles and Strings, and Cluster Algebras,” [arXiv:1912.11764 \[hep-th\]](#).
- [10] D. Damgaard, L. Ferro, T. Lukowski, and M. Parisi, “The Momentum Amplituhedron,” *JHEP* **08** (2019) 042, [arXiv:1905.04216 \[hep-th\]](#).
- [11] Y.-t. Huang, R. Kojima, C. Wen, and S.-Q. Zhang, “The orthogonal momentum amplituhedron and ABJM amplitudes,” *JHEP* **01** (2022) 141, [arXiv:2111.03037 \[hep-th\]](#).
- [12] S. He, C.-K. Kuo, and Y.-Q. Zhang, “The momentum amplituhedron of SYM and ABJM from twistor-string maps,” *JHEP* **02** (2022) 148, [arXiv:2111.02576 \[hep-th\]](#).
- [13] S. He, C.-K. Kuo, Z. Li, and Y.-Q. Zhang, “All-Loop Four-Point Aharony-Bergman-Jafferis-Maldacena Amplitudes from Dimensional Reduction of the Amplituhedron,” *Phys. Rev. Lett.* **129** no. 22, (2022) 221604.
- [14] K. Hosomichi, K.-M. Lee, S. Lee, S. Lee, and J. Park, “N=5,6 Superconformal Chern-Simons Theories and M2-branes on Orbifolds,” *JHEP* **09** (2008) 002, [arXiv:0806.4977 \[hep-th\]](#).
- [15] O. Aharony, O. Bergman, D. L. Jafferis, and J. Maldacena, “N=6 superconformal Chern-Simons-matter theories, M2-branes and their gravity duals,” *JHEP* **10** (2008) 091, [arXiv:0806.1218 \[hep-th\]](#).

- [16] S. He, Y.-t. Huang, and C.-K. Kuo, “The ABJM Amplituhedron,” [arXiv:2306.00951 \[hep-th\]](#).
- [17] N. Arkani-Hamed, J. Henn, and J. Trnka, “Nonperturbative negative geometries: amplitudes at strong coupling and the amplituhedron,” *JHEP* **03** (2022) 108, [arXiv:2112.06956 \[hep-th\]](#).
- [18] L. F. Alday, E. I. Buchbinder, and A. A. Tseytlin, “Correlation function of null polygonal Wilson loops with local operators,” *JHEP* **09** (2011) 034, [arXiv:1107.5702 \[hep-th\]](#).
- [19] O. T. Engelund and R. Roiban, “On correlation functions of Wilson loops, local and non-local operators,” *JHEP* **05** (2012) 158, [arXiv:1110.0758 \[hep-th\]](#).
- [20] O. T. Engelund and R. Roiban, “Correlation functions of local composite operators from generalized unitarity,” *JHEP* **03** (2013) 172, [arXiv:1209.0227 \[hep-th\]](#).
- [21] L. F. Alday, P. Heslop, and J. Sikorowski, “Perturbative correlation functions of null Wilson loops and local operators,” *JHEP* **03** (2013) 074, [arXiv:1207.4316 \[hep-th\]](#).
- [22] L. F. Alday, J. M. Henn, and J. Sikorowski, “Higher loop mixed correlators in N=4 SYM,” *JHEP* **03** (2013) 058, [arXiv:1301.0149 \[hep-th\]](#).
- [23] J. M. Henn, G. P. Korchemsky, and B. Mistlberger, “The full four-loop cusp anomalous dimension in $\mathcal{N} = 4$ super Yang-Mills and QCD,” *JHEP* **04** (2020) 018, [arXiv:1911.10174 \[hep-th\]](#).
- [24] D. Chicherin and J. M. Henn, “Symmetry properties of Wilson loops with a Lagrangian insertion,” *JHEP* **07** (2022) 057, [arXiv:2202.05596 \[hep-th\]](#).
- [25] S. He, C.-K. Kuo, Z. Li, and Y.-Q. Zhang, “Emergent unitarity, all-loop cuts and integrations from the ABJM amplituhedron,” *JHEP* **07** (2023) 212, [arXiv:2303.03035 \[hep-th\]](#).
- [26] J. M. Henn, M. Lagares, and S.-Q. Zhang, “Integrated negative geometries in ABJM,” [arXiv:2303.02996 \[hep-th\]](#).
- [27] L. F. Alday and J. M. Maldacena, “Gluon scattering amplitudes at strong coupling,” *JHEP* **06** (2007) 064, [arXiv:0705.0303 \[hep-th\]](#).
- [28] L. F. Alday and J. Maldacena, “Comments on gluon scattering amplitudes via AdS/CFT,” *JHEP* **11** (2007) 068, [arXiv:0710.1060 \[hep-th\]](#).
- [29] L. F. Alday and J. Maldacena, “Null polygonal Wilson loops and minimal surfaces in Anti-de-Sitter space,” *JHEP* **11** (2009) 082, [arXiv:0904.0663 \[hep-th\]](#).
- [30] A. Brandhuber, P. Heslop, and G. Travaglini, “MHV amplitudes in N=4 super Yang-Mills and Wilson loops,” *Nucl. Phys. B* **794** (2008) 231–243, [arXiv:0707.1153 \[hep-th\]](#).
- [31] J. M. Drummond, G. P. Korchemsky, and E. Sokatchev, “Conformal properties of four-gluon planar amplitudes and Wilson loops,” *Nucl. Phys. B* **795** (2008) 385–408, [arXiv:0707.0243 \[hep-th\]](#).
- [32] J. Drummond, J. Henn, G. Korchemsky, and E. Sokatchev, “On planar gluon amplitudes/Wilson loops duality,” *Nucl. Phys. B* **795** (2008) 52–68, [arXiv:0709.2368 \[hep-th\]](#).
- [33] J. M. Drummond, J. Henn, G. P. Korchemsky, and E. Sokatchev, “The hexagon Wilson loop and the BDS ansatz for the six-gluon amplitude,” *Phys. Lett. B* **662** (2008) 456–460, [arXiv:0712.4138 \[hep-th\]](#).

- [34] J. M. Drummond, J. Henn, G. P. Korchemsky, and E. Sokatchev, “Hexagon Wilson loop = six-gluon MHV amplitude,” *Nucl. Phys. B* **815** (2009) 142–173, [arXiv:0803.1466 \[hep-th\]](#).
- [35] Z. Bern, L. Dixon, D. Kosower, R. Roiban, M. Spradlin, C. Vergu, and A. Volovich, “The Two-Loop Six-Gluon MHV Amplitude in Maximally Supersymmetric Yang-Mills Theory,” *Phys. Rev. D* **78** (2008) 045007, [arXiv:0803.1465 \[hep-th\]](#).
- [36] S. Caron-Huot, “Notes on the scattering amplitude / Wilson loop duality,” *JHEP* **07** (2011) 058, [arXiv:1010.1167 \[hep-th\]](#).
- [37] L. J. Mason and D. Skinner, “The Complete Planar S-matrix of N=4 SYM as a Wilson Loop in Twistor Space,” *JHEP* **12** (2010) 018, [arXiv:1009.2225 \[hep-th\]](#).
- [38] D. Chicherin and J. Henn, “Pentagon Wilson loop with Lagrangian insertion at two loops in $\mathcal{N} = 4$ super Yang-Mills theory,” *JHEP* **07** (2022) 038, [arXiv:2204.00329 \[hep-th\]](#).
- [39] W.-M. Chen and Y.-t. Huang, “Dualities for Loop Amplitudes of N=6 Chern-Simons Matter Theory,” *JHEP* **11** (2011) 057, [arXiv:1107.2710 \[hep-th\]](#).
- [40] S. Caron-Huot and J. M. Henn, “Iterative structure of finite loop integrals,” *JHEP* **06** (2014) 114, [arXiv:1404.2922 \[hep-th\]](#).
- [41] D. Simmons-Duffin, “Projectors, Shadows, and Conformal Blocks,” *JHEP* **04** (2014) 146, [arXiv:1204.3894 \[hep-th\]](#).
- [42] A. Hodges, “Eliminating spurious poles from gauge-theoretic amplitudes,” *JHEP* **05** (2013) 135, [arXiv:0905.1473 \[hep-th\]](#).
- [43] H. Elvang, Y.-t. Huang, C. Keeler, T. Lam, T. M. Olson, S. B. Roland, and D. E. Speyer, “Grassmannians for scattering amplitudes in 4d $\mathcal{N} = 4$ SYM and 3d ABJM,” *JHEP* **12** (2014) 181, [arXiv:1410.0621 \[hep-th\]](#).
- [44] N. Gromov and P. Vieira, “The all loop AdS4/CFT3 Bethe ansatz,” *JHEP* **01** (2009) 016, [arXiv:0807.0777 \[hep-th\]](#).
- [45] N. Gromov and A. Sever, “Analytic Solution of Bremsstrahlung TBA,” *JHEP* **11** (2012) 075, [arXiv:1207.5489 \[hep-th\]](#).
- [46] N. Beisert, B. Eden, and M. Staudacher, “Transcendentality and Crossing,” *J. Stat. Mech.* **0701** (2007) P01021, [arXiv:hep-th/0610251](#).
- [47] L. Griguolo, D. Marmiroli, G. Martelloni, and D. Seminara, “The generalized cusp in ABJ(M) N = 6 Super Chern-Simons theories,” *JHEP* **05** (2013) 113, [arXiv:1208.5766 \[hep-th\]](#).
- [48] M. Lagares and S.-Q. Zhang, “Higher-loop integrated negative geometries in ABJM,”.